Analysis of Star Formation Main Sequences based on IllustrisTNG Simulations

Yongquan Hu *

School of Physics, University of Science and Technology of China, Hefei, China

* Corresponding author: frank_hu_2020@mail.ustc.edu.cn

Abstract. As a matter of fact, N body simulations are widely used in cosmology and astrophysics. Thanks to the rapid development of computer resources, it is available to carry out galaxy simulations including magnetic evolution, for example, the project of IllustrisTNG and THESAN. In this case, based on the data collected from IllustrisTNG API, investigations into the star formation main sequence (SFMS) of dark matter (DM) halos are carried out by querying the accomplished simulation tasks. To be specific, multiple linear relation among the star formation rate (SFR) of DM halos, the stellar mass of DM halos and cosmological red shift are discovered. According to the analysis, a polynomial relation between the SFR and the stellar mass of DM halos is revealed, in which the coefficients are related to the redshift. Overall, these results shed light on guiding further exploration of star and galaxy formation based on analysis of the simulation results.

Keywords: Star formation, IllustrisTNG, cosmology simulations.

1. Introduction

A well-established theory called the Λ cold dark matter (ΛCDM) paradigm explains that, as the Universe ages and expands, galaxies build up in DM halos due to the uneven distribution of matter in the early Universe [1]. Related simulations have been done, utilizing a model of particles with gravity to describe the behavior of DM [2-4]. These simulations showed several typical patterns of the distribution and evolution of DM in the DM halos.

While gained a fairly thorough understanding of how DM evolves, little do mankind knows about the evolution and formation of the baryon part of DM halos. Thus, scholars never stopped researching into this subject. Theories of star and galaxy formation have been brought up [5-7], and observations about morphologies and formation laws of stars as well as galaxies have been done [8-11]. A few years ago, the idea of SFMS was raised [12]. The tactfully established SFMS reveals a tight relation between the SFR and the stellar mass of galaxies that are conceiving new stars, and it applies to a wide range of redshift (0<z<6, where z denotes the cosmological redshift) [13, 14]. A linear relation was also found between the SFR and the stellar mass of galaxies at redshift of around 1 and below [13, 15, 16].

In this paper, a linear relation between the logarithm of SFR and the logarithm of stellar mass of DM halos (so-called “subhalos” in Illustris simulations) is found using simulation data from Illustris-3. According to the analytical result, this relation applies to an even wider range of redshift (0<z<10). Relation between the linear coefficients and redshift is then further investigated. Results in this paper is trustable because similar analysis about SFMS in Illustris simulations has been done before [17].

2. Data and Method

This paper uses part of Illustris-3 simulation results collected from IllustrisTNG API using Python code [18]. SFR and stellar mass of all subhalos in each snapshot is collected and properly processed. There are over 5,000,000 pieces of SFR and stellar mass data, and 136 snapshots of the simulated Universe at different redshift in total. When organizing the collected data, it was easy to realize that most subhalos have stellar mass of $10^{10} \sim 10^{12}\ M_{Sun}$, where M_{Sun} denotes the mass of the Sun. For example, in snapshot No. 125 ($z = 0.1258$), of all 123933 subhalos, up to 91.6% have stellar mass that is distributed between $10^{10} \sim 10^{12}\ M_{Sun}$. Data about SFR, stellar mass and mass distribution of subhalos in snapshot No. 125 is shown in the Fig. 1, where M_G denotes the sum of stellar mass of all the galaxies in a subhalo. Thus, in this paper, only subhalos that have stellar mass of 10^{10}~10^{12} M_{Sun} are taken account of. This approach proves to be effective in cancelling noise data while analysing. Linear fitting method is used in all analyses in this paper. As for non-linear relations, logarithm or reciprocal of certain variables are derived to form linear relations. All these analyses are done with the help of numpy.polyfit() function in NumPy Python package [19].

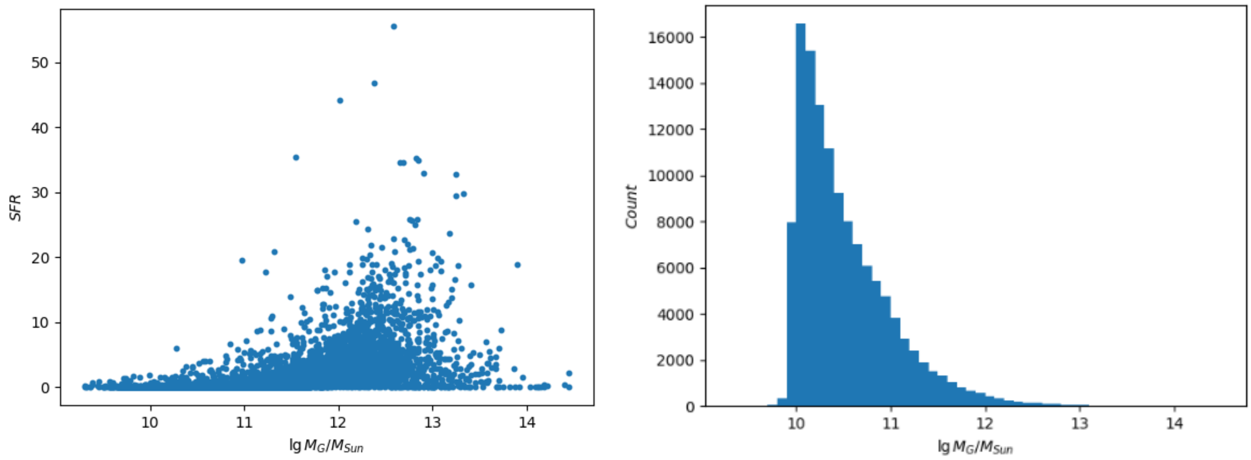

Figure 1. Data of subhalos in snapshot No. 125.

3. Relation between SFR and Subhalo Mass

As one can see in the example of snapshot No. 125, there are over 100,000 subhalos in it, meaning that there are over 100,000 points in Fig. 1. Troubles were encountered when analysing such huge data, and the relation between SFR and subhalo mass was not easy to find. Another approach of processing the data is applied. Firstly, subhalos with stellar mass under 10^{10} M_{Sun} or over 10^{12} M_{Sun} are excluded. Then, an approach of dividing the x-axis (which stands for $\lg \mathrm{M_G}/\mathrm{M_{Sun}}$) into small, equal-length intervals is applied to deal with the data. In this paper, each interval has a length of 0.1. All subhalos located in each interval generate a mean value of SFR according to the formula:

$$SFR_i = \frac{1}{N_i} \sum_{\substack{10+0.1i \\ <\lg M_{Gj}/M_{Sun} \\ <10+0.1(i+1)}} SFR_j\,,\ 0 \le i < 20, \tag{1}$$

Where SFR_i and N_i denote the mean SFR and the count of all subhalos in the i'th interval, M_{Gj} and SFR_j denote the stellar mass and the SFR of j'th subhalo in the i'th interval. The Fig. 2 shows the processed data of snapshot No. 125.

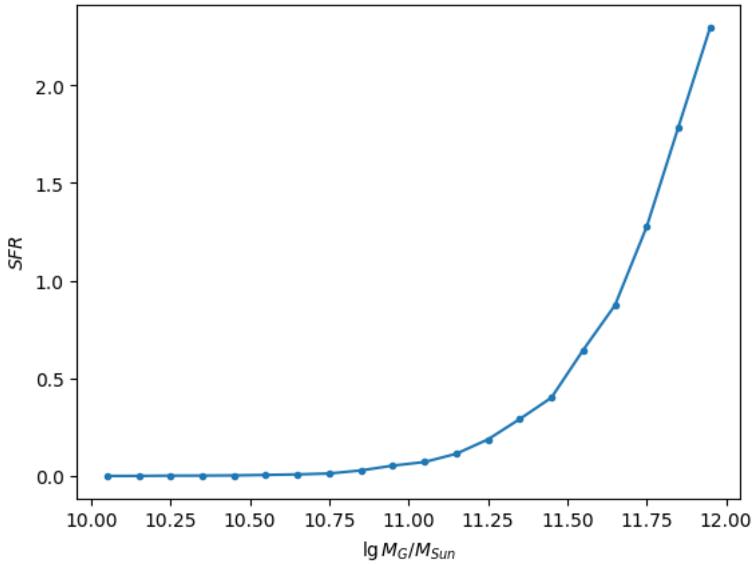

Figure 2. Processed data of snapshot No. 125

After the preliminary processing, the natural logarithms of all the mean SFR values are derived. This operation is based on the knowledge of the linear relation between the SFR and the stellar mass of galaxies around and under redshift $z = 1$ [13, 15, 16]. Then, linear fitting of $log\,SFR$ and $\lg \mathrm{M_G}/\mathrm{M_{Sun}}$ is applied according to the equation

$$log\,SFR = \alpha\, lg(M_G/M_{Sun}) + \beta, \tag{2}$$

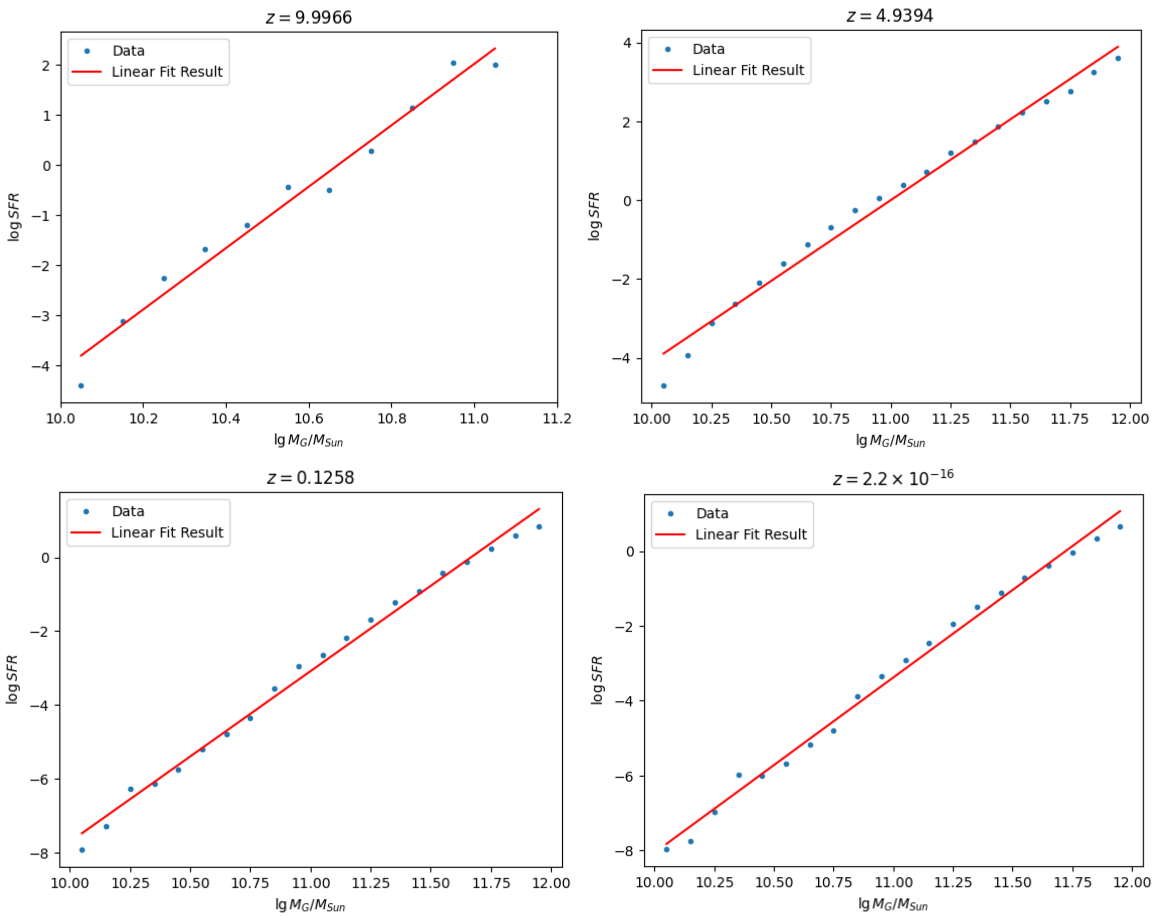

Figure 3. Linear fitting results of four typical examples

Where α and β are two coefficients to be determined. Fitting results illustrated in Fig. 3 show that in a range of redshift as wide as $0 < z < 10$, $log\,SFR$ is linearly related to $\lg M_G/M_{Sun}$, which means that in this range of redshift, SFR is related to stellar mass in a polynomial manner. Linear fitting results of snapshot No. 32 ($z = 9.9966$), No. 50 ($z = 4.9394$), No. 125 ($z = 0.1258$) and No. 135 ($z = 2.2 \times 10^{-16}$) are shown below as four typical examples. Fitting coefficients α and β of the four examples are listed in the Table 1.

Table 1. Fitting coefficients of the four examples

Snapshot No.	z	α	β
32	9.9966	6.1 ± 0.3	-65 ± 3
50	4.9394	4.1 ± 0.1	-45 ± 1
125	0.1258	4.6 ± 0.1	-54 ± 1
135	2.2×10^{-16}	4.7 ± 0.1	-55 ± 1

From the fitting equation, one can get the relation between SFR and M_G as below

$$SFR = e^{\beta} \left(\frac{M_G}{M_{Sun}}\right)^{\frac{\alpha}{log\,10}}, \tag{3}$$

Which Is a polynomial relation. It can be further confirmed that, for snapshots at around $z = 2$, α reaches its minimum value of about 3.6 (take snapshot No. 68 for example, $z = 2.0020$, $\alpha = 3.62 \pm 0.05$). At around this redshift, the exponent of M_G on the right side of the equation equals approximately to 1.5, which is rather close to the linear relation between SFR and stellar mass mentioned in the Introduction part. However, 1.5 is still not close enough to 1. Besides, when redshift drops below 2, the exponent of M_G continues to rise, driving the relation even farther away from linear. This is possibly because of the difference between galaxies and subhalos, which are two very distinct astronomical structures.

4. Relation between Coefficients α, β and Redshift

Plotting the relation between α, β and redshift, it's easy to notice that α reaches its minimum and β reaches its maximum at the same time, when redshift is around $z = 2$. In fact, there are only 104 points in each plot of Fig. 4. Though data of 136 snapshots was collected. This is because when redshift is very high ($z > 10$), it means that the Universe is not aged enough to form structures like stars, galaxies or subhalos. In this paper, only snapshots that contains enough subhalos (about 1,000 and above) are taken account of.

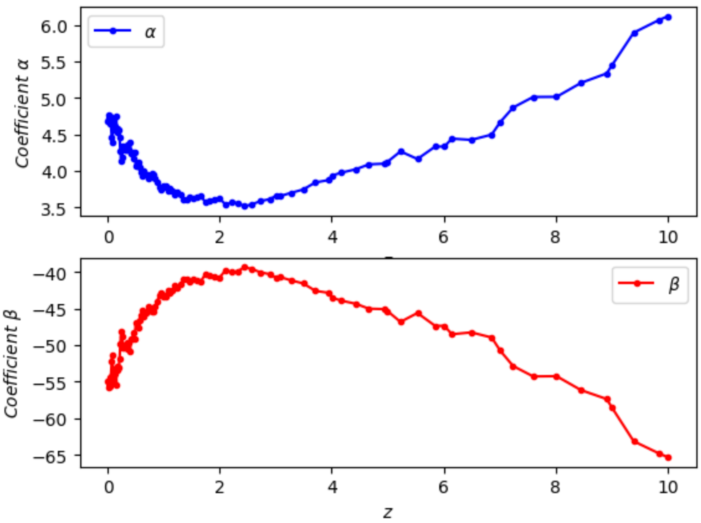

Figure 4. Plotted relation between α, β and redshift

Minimum value of α occurs precisely at $z_m = 2.4442$. It's not hard to notice that when $z > z_m$, relation between the coefficients α, β and redshift tends to be linear; when $z < z_m$, the relation tends to be reciprocal. Thus, linear fitting without and with deriving the reciprocal of the coefficients are applied to the two cases of $z > z_m$ and $z < z_m$ respectively, according to the fitting equations (4) and (5)

$$\alpha = A_1 z + B_1,\ \beta = A_2 z + B_2, \tag{4}$$

$$\alpha^{-1} = A_3 z + B_3,\ \beta^{-1} = A_4 z + B_4, \tag{5}$$

Where $A_1 \sim A_4$ and $B_1 \sim B_4$ are coefficients to be determined. Fitting results are shown in the Fig. 5 and Table. 2.

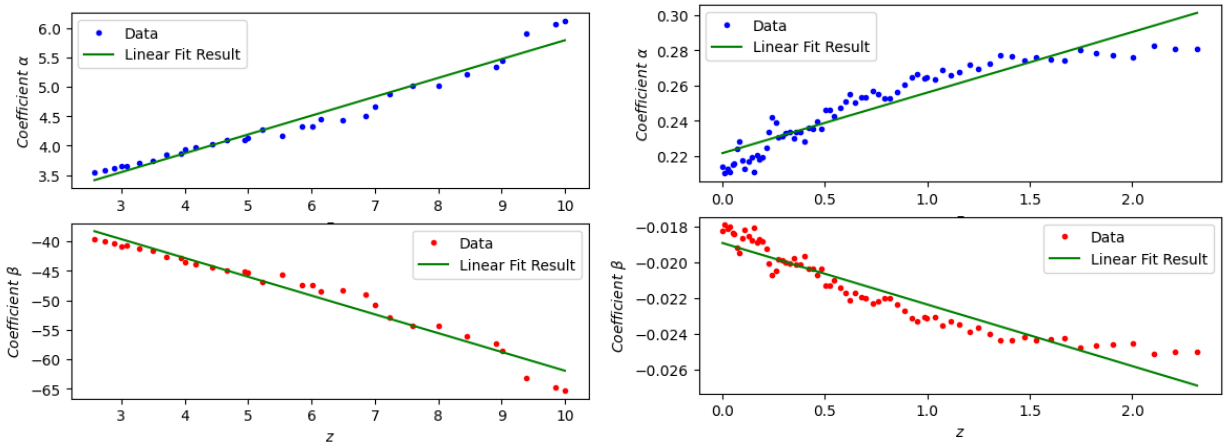

Figure 5. Fitting results at $z > z_m$ (left panel) and $z < z_m$ (right panel).

Table 2. Fitting results at $z > z_m$ and $z < z_m$

A_1	B_1	A_2	B_2
$\mathbf{0.32 \pm 0.01}$	2.6 ± 0.1	-3.2 ± 0.1	-30 ± 1
A_3	B_3	A_3	B_3
$\mathbf{0.0345 \pm 0.0016}$	0.2215 ± 0.0015	-0.0036 ± 0.0001	-0.0189 ± 0.0001

The results fit well, though there is not a good reason why reciprocal of α and β are derived at $z < z_m$. This operation is purely experiential. Another problem is that, it's still ambiguous how SFR actually relates to redshift. To show the actual relation between SFR and redshift, a certain M_G ($M_G = 5 \times 10^{11} M_{Sun}$, which is approximately the same order of the mass of Milky Way [20]) is selected and applied to equation (3) with changing α and β, as in

$$SFR(z) = e^{\beta(z)} \left(\frac{M_G}{M_{Sun}}\right)^{\frac{\alpha(z)}{\log 10}}. \tag{6}$$

Plotted relation between SFR and z is shown in the Fig. 6. Linear fitting results of $\log SFR$ and z are shown in the Fig. 7 and Table. 3. The fitting equation is

$$\log SFR = C_1 z + C_2, \tag{7}$$

Where C_1 and C_2 are coefficients to be determined.

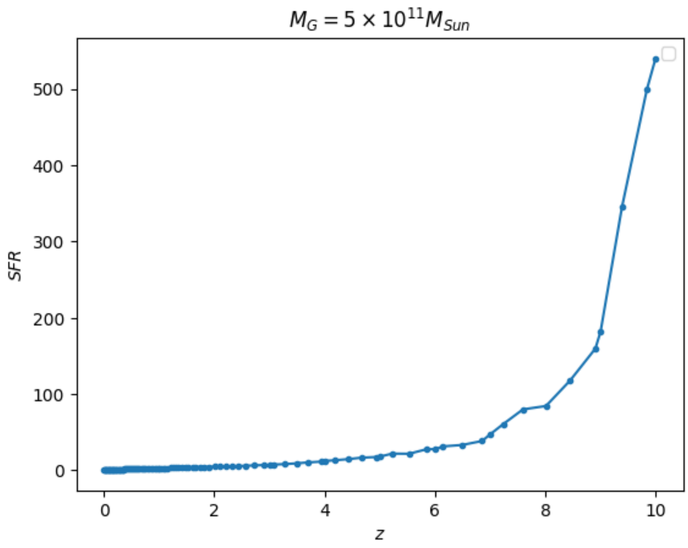

Figure 6. Plotted relation between SFR and redshift.

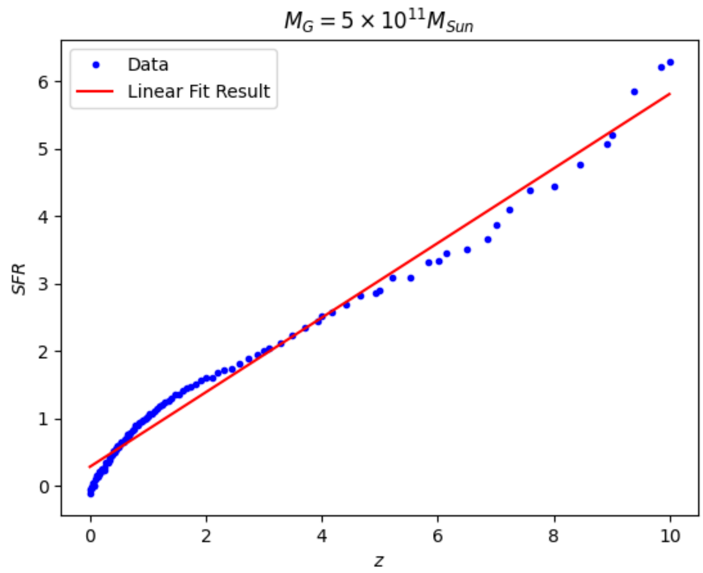

Figure 7. Linear fitting results of SFR and z.

Table 3. Linear fitting results of SFR and z

C_1	C_2
0.55 ± 0.01	0.28 ± 0.03

5. Conclusion

In summary, the relation between the SFR and the stellar mass of subhalos are investigated, as well as the relation between linear fitting coefficients α, β and redshift, and the relation between SFR and redshift. In a range of redshift $0 < z < 10$, linear relations between $log\, SFR$ and $\lg \mathrm{M_G/M_{Sun}}$, coefficients (α and β) and redshift at $z > z_m$, reciprocals of coefficients (α_{-1} and β_{-1}) and redshift at $z < z_m$, $log\, SFR$ and redshift are discovered respectively. The discovered linear relations further revealed a polynomial relation between SFR and stellar mass of subhalos. The investigations above provide an insight into SFMS of DM halos.

References

[1] Zel'dovich Y B. Gravitational instability: An approximate theory for large density perturbations. Astronomy and Astrophysics, 1970, 5: 84 - 89.

[2] Klypin A A, Trujillo-Gomez S, Primack J. Dark Matter Halos in the Standard Cosmological Model: Results from the Bolshoi Simulation. The Astrophysical Journal, 2011, 740 (2): 17.

[3] Springel V, White S D M, Jenkins A, et al. Simulations of the formation, evolution and clustering of galaxies and quasars. Nature, 2005, 435 (7042): 629 - 636.

[4] Diemand J, Kuhlen M, Madau P, et al. Clumps and streams in the local dark matter distribution. Nature, 2008, 454: 735 - 738.

[5] White S D M, Rees M J. Core condensation in heavy halos: a two-stage theory for galaxy formation and clustering. Monthly Notices of the Royal Astronomical Society, 1978, 183 (3): 341 - 358.

[6] Silk J. On the fragmentation of cosmic gas clouds. I. The formation of galaxies and the first generation of stars. Astrophysical Journal, 1977, 211: 638 - 648.

[7] Rees M J, Ostriker J P. Cooling, dynamics and fragmentation of massive gas clouds: clues to the masses and radii of galaxies and clusters. Monthly Notices of the Royal Astronomical Society, 1977, 179: 541 - 559.

[8] Schmidt M. The Rate of Star Formation. Astrophysical Journal, 1959, 129: 243.

[9] Kennicutt, R C Jr. The Global Schmidt Law in Star-forming Galaxies. The Astrophysical Journal, 1998, 498 (2): 541 - 552.

[10] Hubble E P. Extragalactic nebulae. Astrophysical Journal, 1926, 64: 321 - 369.

[11] Dressler A. Galaxy morphology in rich clusters: implications for the formation and evolution of galaxies. Astrophysical Journal, 1980, 236: 351 - 365.

[12] Brown L M, Pais A, Pippard A B. Twentieth century physics. Institute of Physics Pub., American Institute of Physics PressBristol, Philadelphia, 1995: 1696.

[13] Brinchmann J, Charlot S, White S D M, et al. The physical properties of star-forming galaxies in the low-redshift Universe. Monthly Notices of the Royal Astronomical Society, 2004, 351 (4): 1151 - 1179.

[14] Popesso P, Concas A, Cresci G, et al. The Main Sequence of star-forming galaxies across cosmic times. arXiv: 2022, 2203.10487.

[15] Salim S, Rich R M, Charlot S, et al. UV Star Formation Rates in the Local Universe. The Astrophysical Journal Supplement Series, 2008, 173 (2): 267 - 292.

[16] Daddi E, Dickinson M, Morrison G, et al. Multiwavelength Study of Massive Galaxies at z~2. I. Star Formation and Galaxy Growth. The Astrophysical Journal, 2007, 670 (1): 156 - 172.

[17] Sparre M, Hayward C C, Springel V, et al. The star formation main sequence and stellar mass assembly of galaxies in the Illustris simulation. Monthly Notices of the Royal Astronomical Society, 2015, 447 (4): 3548 - 3563.

[18] Illustris project, Public Data Access: Web API Documentation. Retrieved from: https://www.illustris-project.org/data/docs/api/.

[19] NumPy documentation, numpy. polyfit, NumPy v1.25 Manual. Retrieved from: https://numpy.org/doc/stable/reference/generated/numpy.polyfit.html.

[20] Kafle P R, Sharma S, Lewis G F, Bland-Hawthorn, J. Kinematics of the Stellar Halo and the Mass Distribution of the Milky Way Using Blue Horizontal Branch Stars. The Astrophysical Journal, 2012, 761 (2): 17.